Development and Applications of LDA-Systems in I.C. Engine Research

F.Durst, A.Naqwi and C.Tropea

Lehrstuhl für Strömungsmechanik
Universität Erlangen/Nürnberg
Cauerstrasse 4
8520 Erlangen
F.R.Germany

ABSTRACT

The present paper summarizes development work that has been performed at the authors' laboratory at the University of Erlangen/Nuremberg in the field of laser-Doppler and phase-Doppler anemometry and its application to flows related to internal combustion engines. A fiber optic LDA is described and it is shown that this set-up reduces the alignment efforts, necessary for in-cylinder velocity measurements. It also reduces on-site preparations of the measuring technique. The fiber probe uses graded index fibers that are aligned to be excited in their fundamental mode for beam transmission. It is shown that the probe provides a high degree of robustness and good temporal stability of the alignment.

The paper also summarizes development work on small LDA-systems utilizing semi-conductor lasers and photodetectors. Utilizing semi-conductor elements allows the size of laser-Doppler probes to be reduced considerably. Since semi-conductor lasers require low electrical power, systems result that can be used for measurements in moving automobiles. Developments and applications of phase-Doppler anemometer systems are summarized and their application to sprays is described. From these measurements, size and velocity distributions result that require drastic data reduction to yield information that can readily be used to interpret the physical contents of the measurements and to use this information for improved spray nozzle design.

1. INTRODUCTION

Recently, there has been a keen interest in the knowledge of mean flow and turbulence intensity inside the cylinder of internal combustion engines, as these parameters seem to have a strong influence on the performance of the engines. This has led to increased efforts to apply laser-Doppler anemometers for velocity and turbulence measurements in engines. A number of studies are available in which extensive measurements of this kind are documented for both motored and fired research and production engines. Most of these measurements employ conventional, modular LDA-systems, see ref. /1-6/. Such systems are large in size and and also have large space requirements around the internal combustion engines. To reduce the size of the equipment required close to the engine, glass fiber optical probes have been built and used. The present paper describes such a probe and its application for in-cylinder velocity measurements.

Fiber optical probes have found limited use to-date in this field, partly due to the high precision required in coupling alignment, and partly due to limited power transmission levels through fibers. However, both of these aspects have been improved upon recently in commercially available fiber optical LDA-systems /7,8/. Obokata et al. /9/ have demonstrated the use of a fiber optical transmission optics with a conventional receiving system in forward scatter, used for both motored and fired conditions. A variety of fiber optical sensor designs have been introduced by Durst et al. /10/ employing graded index fibers, however these have not been used for extensive engine measurements. Their employment for such measurements is described in this paper. It is shown that good measurements can be obtained and the small probe size simplifies the traversing of the measuring volume to yield velocity distributions inside the internal combustion engines.

The availability of monomode laser diodes with high coherence length in combination with avalanche photodiodes and pindiodes is promoting the development of a new generation of laser-Doppler anemometers /11-14/. These systems — based on semi-conductor lasers and detectors — consume less electrical power and have the advantage of being small in size and relatively inexpensive to built. Development work using these elements has been carried out at LSTM-Erlangen and these suggest that LDA-systems based on semi-conductor lasers and photodetectors may be used in many new applications, such as studies of internal combustion engines and their performance in driving cars. However, previously reported measurements with semi-conductor LDA-systems have shown high inaccuracies in the rms-levels of the signals; the variance of the measured data has been rather large. A drift in the calibration has also been noticed. However, reliable layouts of semi-conductor LDA-systems can be made and have been demonstrated to yield precise laser-Doppler measurements, comparable with those obtained with gas lasers and photomultipliers.

The present paper also describes phase-Doppler systems and their application to liquid sprays. It is shown that these instruments result in a large number of measurements of size and velocity distributions that cannot be used for engineering considerations to yield improved spray nozzle designs. It is therefore suggested to utilize log-hyperbolic distributions to match the measured particle sizes and to use the parameters of the log-hyperbolic functions to characterize the particle size distributions. This yields four parameters, whose spatial distribution

is used to describe the entire set of particle size distributions. Extensions of this work, to characterize the joint distributions of size and velocity using log-hyperbolic functions, are underway.

2. FIBER OPTIC LDA SYSTEMS

The optical system designed for LDA-measurements in IC-engines is shown schematically in Fig. 1. A 4W Ar-Ion laser (1) operating without an etalon provides a light source which is first split into two beams of equal intensity using a Bragg cell (2), the first order beam being shifted 40 MHz from the zeroth order beam. A two lens collimator (3) then follows, placing the beam waist at the face of the fiber input couplers and with a waist diameter of 250 μm. The Amici-prism (4) then splits the two beams into their separate colours of which the 488 nm and 514.5 nm lines are caught by mirrors (5) & (6) and forwarded to the coupling optics (7). These consist of the narrow type SELFOC rod lenses butted directly against the polished face of a 50/125 μm graded-index (GRIN) fiber (8). Each of the four couplers allow two translation directions and two tilt adjustments, the latter being the more sensitive for optimizing transmission efficiency. The system is laid out to keep the focussed beam waist at the back face of the SELFOC lens smaller than the characteristic spot size of the fiber, in this case 4.406 μm for 488 nm and 4.524 μm for 514.5 nm. This excites only the fundamental mode of transmission for a Gaussian beam and while other modes develop due to intermodal dispersion, a measurement control volume can be maintained with little adjustment over long periods of time. The overall transmitted power in a single fiber usually exceeds 80% of the input power for input powers up to 1.6 W, whereby polarization is not completely preserved.

A cross-section of the fiber optic probe head is illustrated in Fig. 2, in which the two output coupling microlenses for one of the colours are shown as well as the receiving fiber. Basic dimensions and specifications of the probe are given in Table 1. Special attention must be given to the receiving optics, since the fiber pick-up acts as the only possible spatial filter, in contrast

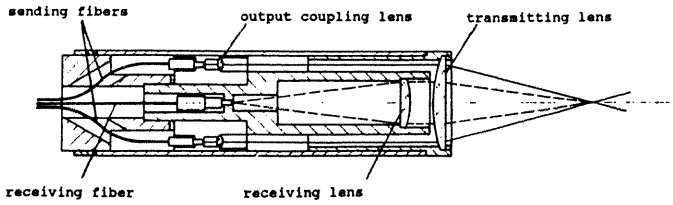

Figure 2: Cross-section of fiber optic probe.

with conventional modular LDA-systems. In the present case, the f-number of the receiving aperture is 4.3 and the magnification is 1.25, meaning that the control volume image on the face of the 50 μm diameter receiving fiber core is 62 μm.

To evaluate the design parameters of the probe a Mie scattering computation was performed, comparing at the same time a number of other typical modular LDA-systems, also listed in Table 1. The computations took into account the beam expansion and hence the light intensity in the control volume, as well as the collection aperture. The results are shown in Fig. 3, indicating that, while the fiber optic probe falls below other optical systems in the submicron size range shown, the fluctuations due to size variation are in general larger than the differences in systems. Typically, commercial fiber optic probes achieve a smaller f-number than the present probe given equal outer dimensions. This is achieved by providing clearance holes in the receiving lens for the outgoing beams. In the present probe the receiving lens diameter is kept smaller than the beam separation, in fact only to simplify construction.

Referring again to Fig. 1, the received light is passed through a dichroic colour separator (11) and focussed onto two avalanche photodiodes (APD) (12). These are of the selected type displaying a quantum efficiency of over 45% in this spectral range and an internal avalanche gain of up to 250. These units are packaged together with a high gain preamplifier with a system bandwith of 110 MHz. Further details can be found in /15/.

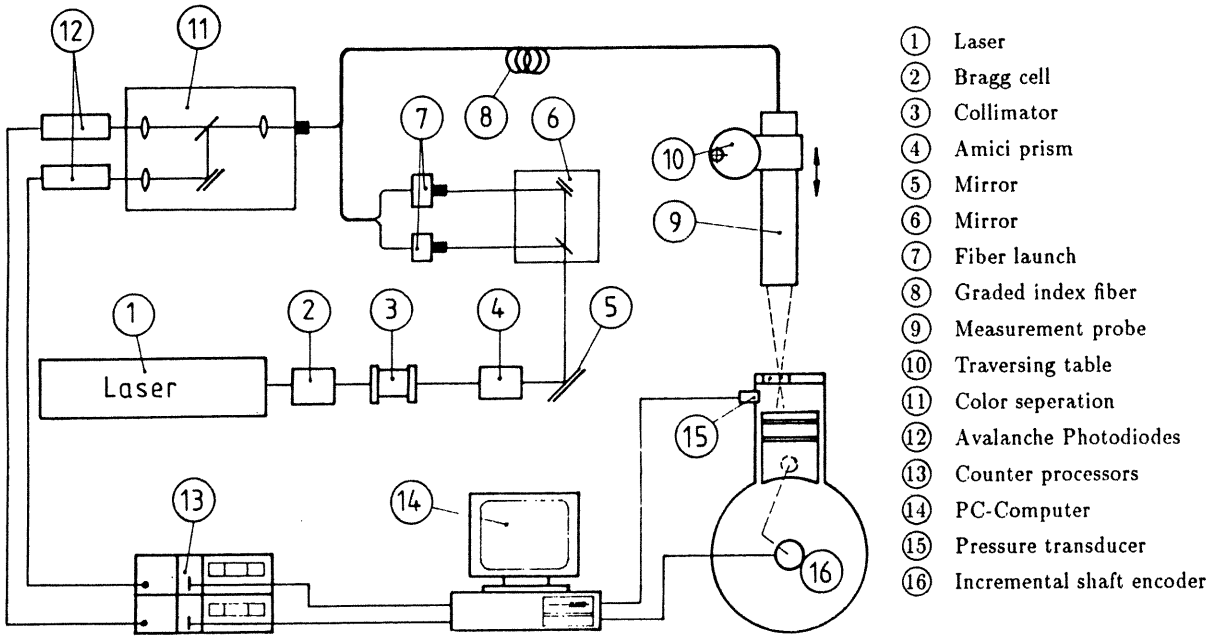

Figure 1: Schematic of optics and electronics for engine measurements.

LDA-Optic	Label in Figure 3	Diameter of probe [mm]	Focal-length [mm]	Intersection half-angle [°]	Receiving half-angle [°]	Control volume diameter [μm]	Control volume length [μm]	Receiving f - number
LSTM fiber probe	LSTM	30	50	11.3	6.56	46	230	4.3
TSI standard optic Type: 9100-6	TSI	83	122	10.75	9.46	59	310	3.05
TSI optic with beam expander 2.27	TSIex	83	122	10.75	9.46	26	136	3.05
DANTEC optic 55X.. beam expander 1.95 IMH-Optic	DANTex	122	160	10.62	20.55	41	218	1.7

Table I: Probe specifications

3. EXPERIMENTAL RESULTS USING FIBER OPTIC LDA

The measurement location and the sign conventions of the velocity components are summarized in Fig. 4. The measurement point lies 5 mm from the access window, about halfway towards the piston at TDC. Radial and tangential velocity components were sequentially acquired, both at the same operating condition of 1000 rpm, half-load and fuel-to-air ratio of 1.0. At these conditions typically 60–80 cycles of data could be acquired in one run, several of which are shown sequentially in Fig. 5.

This figure shows the radial velocity component together with the cylinder pressure taken using a piezoelectric transducer. Both similarities and differences in these sequential cycles are of interest. The difference in the pressure trace, for instance is indicative of strongly varying combustion rates, at least partially attributed to the turbulence characteristics of the combustion chamber flow. In other respects the velocity data are very similar. The intake stroke is characterized by violent velocity fluctuations reducing dramatically during compression and through ignition and burning. The flame passage is usually evident, as is the opening of the exhaust valve. Tangential velocity measurements show similar characteristics.

The time and velocity resolution is better illustrated in Fig. 6, in which the interval 240°–400° is shown in detail. Not only a data rate of 17 kHz is obtained in this interval — which is sufficient to resolve most velocity fluctuations — there appear remarkably few points which seem to be spurious. In fact further processing was performed without altering the raw data files. Note the ensemble mean velocity, obtained over 83 cycles is of little use in describing the instantaneous flow field.

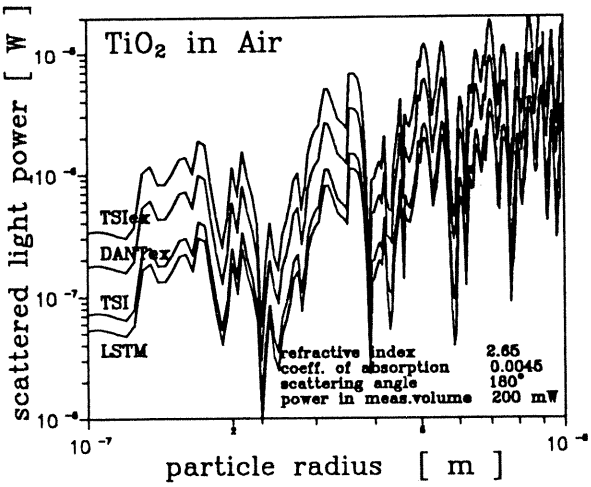

Figure 3: Computed scattering characteristics of optical systems.

The particle arrivals were also analysed in an alternate manner, as shown in Fig. 7. Here the relative probability of another particle arrival within a given angular interval is shown for the entire cycle and for just the ignition-burning interval 240°–400°. Clearly a resolution well above 1° crank angle has been achieved. Again, this result is heavily dependent on proper seeding particle generation and introduction, as outlined in /16/.

For purposes of examining the spectral content of the velocity fluctuations, the random particle arrivals in LDA are not convenient since the FFT algorithm cannot be applied to perform the Fourier transform. Therefore an interval averaging was applied, which averaged all velocity data within a given crank angle interval, producing a series of averaged values equally spaced in crank angle. Fig. 8 illustrates the interval-averaged result compared with the raw data. In the case of no data ap-

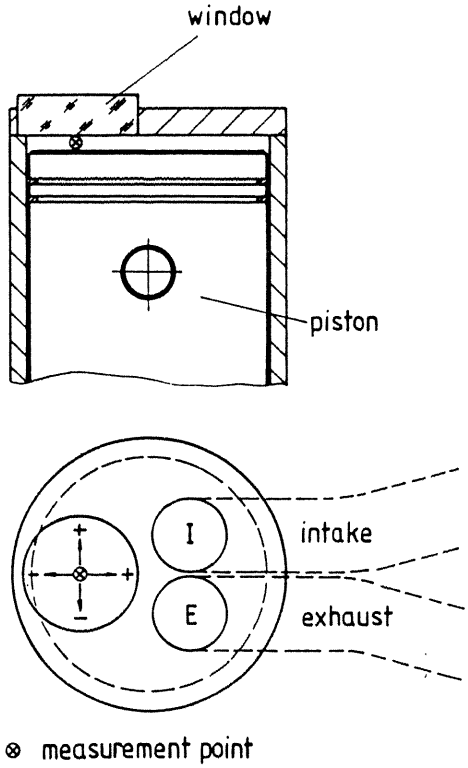

Figure 4: Measurement location and sign convention.

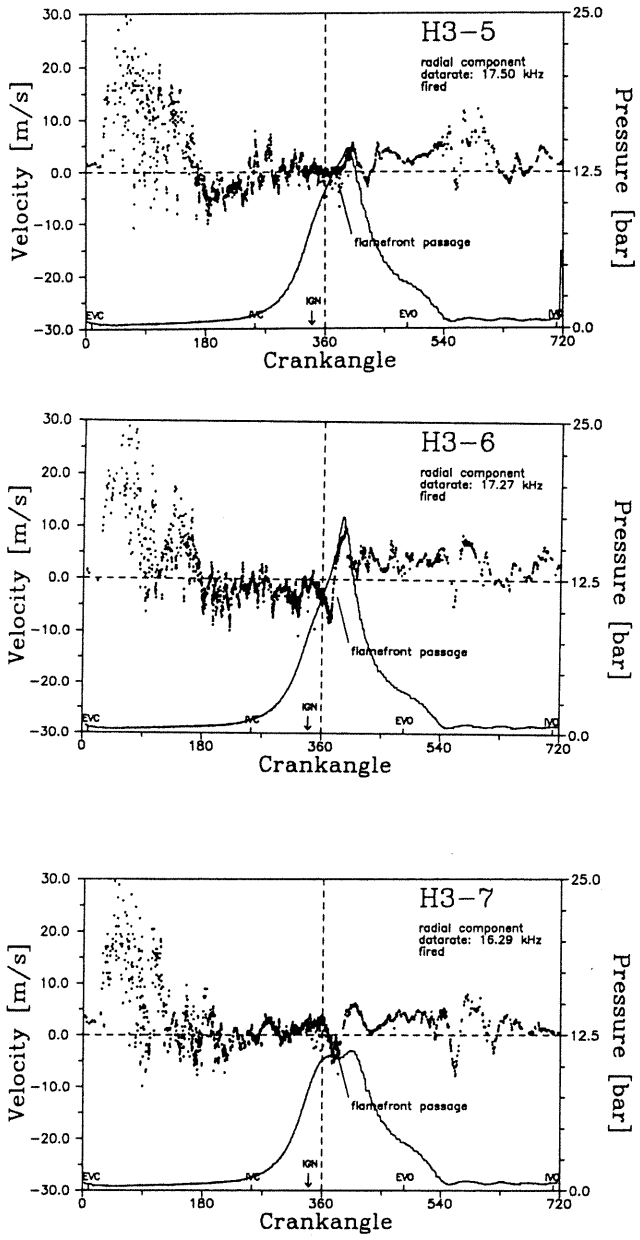

Figure 5: Sequential cycles of radial velocity component.

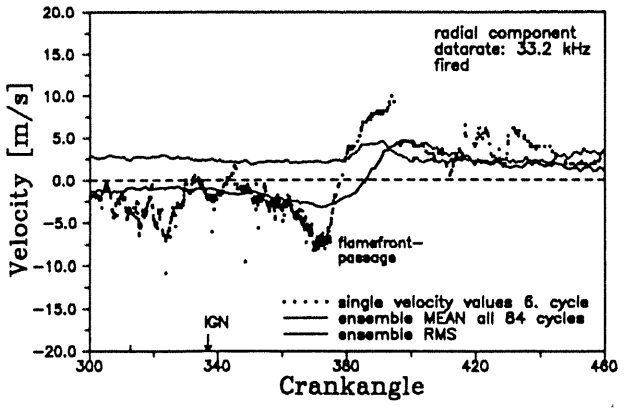

Figure 6: Measured radial velocity in a single cycle over the crank angle interval 300°–460°.

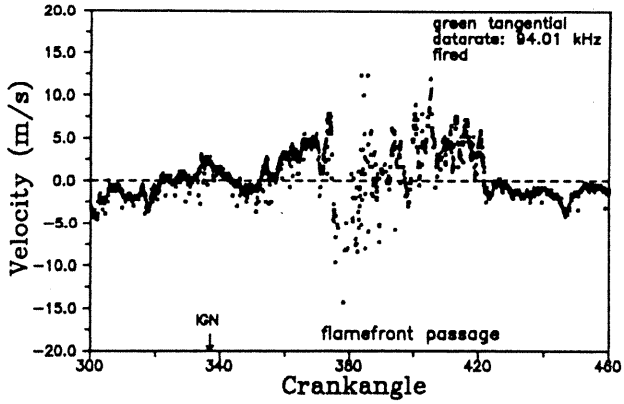

Figure 7: Measured tangential velocity in a single cycle.

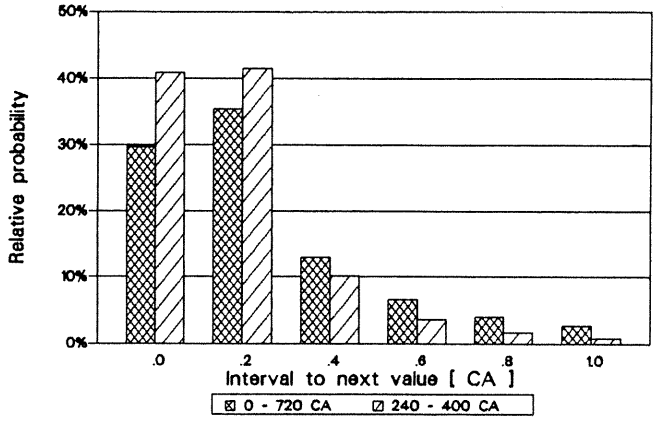

Figure 8: Particle arrival statistics averaged over 84 cycles.

pearing in an interval, which Fig. 7 shows to occur seldom, a linear interpolation is used on the two nearest neighbouring data points.

The velocity time series obtained using this system illustrated clearly the large cyclic variations of the engine and the inherent difficulties with ensemble averaging. Also these variations are clearly present in the cylinder pressure traces. Valve openings and closings are detectable in the velocity traces taken at the chosen measurement location, as is the flame passage over the measurement volume.

4. SEMICONDUCTOR LDA SYSTEM

The present work on semiconductor LDA has shown that the non-uniformity of fringes is the main source of uncertainty in the measurements taken with these instruments. Earlier studies on this effect have been concerned only with Gaussian laser beams /17,18/. A laser diode beam deviates significantly from a Gaussian beam. Furthermore, the error in signal frequency depends not only on the non-uniformity of fringes but also on the method used for processing the non-uniform signals. Only recently, a rigorous analysis of the frequency error in dual-beam LDA has been presented /19/. Based on this analysis, the performance of a semiconductor LDA system was estimated. The data of frequency error were also obtained experimentally with a precision device for scanning the fringes. The experimental data have verified the theoretical predictions.

The LDA system under consideration is shown schematically in Fig. 9. The diverging beam of the laser diode is collimated using a small focal length lens. The axis of polarization of the

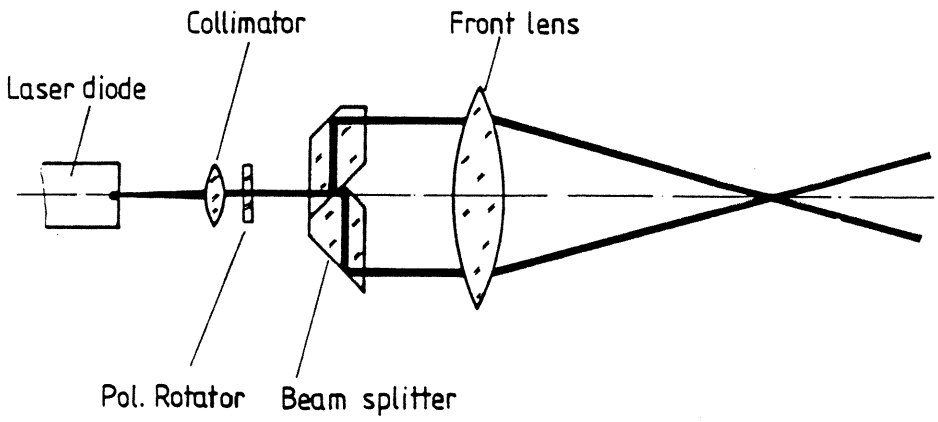

Figure 9: Schematic of semiconductor LDA.

collimated beam is rotated so that it could be split up into two parallel beams of equal intensity and matched polarization. The front lens serves the usual purpose of bending and focusing the two beams so that they intersect at their focal spots. It is desirable that both the beams have plane wavefronts in the region of overlap. However, laser diode beams tend to become non-planar within a short distance from the focal plane, contributing large uncertainties in measurements unless special precautions are taken to suppress this effect. In order to estimate the magnitude of this effect, an analytical description of the optical field in the measuring volume is achieved through the following steps:

- The optical field emerging from the laser diode is mathematically modelled.
- Collimation of the original field is considered as a process which adds a negative curvature to the diverging field. It also truncates the field due to finite numerical aperture of the collimator. Furthermore, phase aberrations are introduced by the collimating lens.
- After collimation, the optical field may be considered paraxial and further propagation may be described by Fresnel integral.

For the present purpose, a monomode laser diode with emitting power upto 50 mW is considered. Such a laser has a stripe-type junction which is about 0.1 μm thick and less than 10 μm wide. The length of the junction is 200–300 μm. The emitted laser beam emerges out of the 0.1 μm × 10 μm cross-section. Typically, the intensity of the diverging beam falls to 50% of the maximum over an angle of 10° in the plane of the junction and 30°–40° normal to it. The optical field distribution along the junction may be considered Gaussian, whereas normal to the junction it may be approximated by Lorentzian distribution.

Starting with the above description of the diode laser beam, the focused fields of the two beams in the measuring volume are computed. In Reference /19/, analytical expressions are given for the Gaussian distribution of the focused field, whereas a computational procedure is suggested for evaluation of the Lorentzian distribution. The knowledge of focused field allows one to simulate the LDA signal and provides an estimate of the signal frequency at individual points in the measuring volume. The time-domain value of the Doppler frequency is estimated by averaging this local frequency along the particle path. In the case of frequency-domain signal processing, the measured frequency corresponds to the peak of the signal spectrum. The peak frequency is generally different from the average frequency. Computations have shown that the average frequency coincides with the peak frequency for an aberration-free LDA system using Gaussian distribution in the plane of beam intersection. However, they are appreciably different if the Lorentzian distribution lies in the plane of the beams. The difference becomes larger if the aberration effects are also included.

In Figs. 10–12, computed values of the relative frequency error, for the present hardware, are given as a function of the normalized distance along the length of the measuring volume. In the case of the Gaussian distribution lying in the plane of beam intersection, the measuring volume length is based on $1/e^2$ intensity points. For Lorentzian distribution, the boundaries of the measuring volume are defined as the points where the amplitude of signal fluctuation reduces to 20% of its value at the center. Each curve in these figures corresponds to a particular collimator position. It may be noticed that a substantial deviation from the nominal frequency may be caused merely by micron-size collimator displacements.

Results in Fig. 10 are valid for both time-domain as well as frequency-domain signal processing. It is obvious that Gaussian distribution yields smaller frequency error than Lorentzian distribution. If the Lorentzian distribution must be used in the plane of beam intersection, it is preferable to perform a spectrum analysis of the signal as it produces better results than time-domain processing.

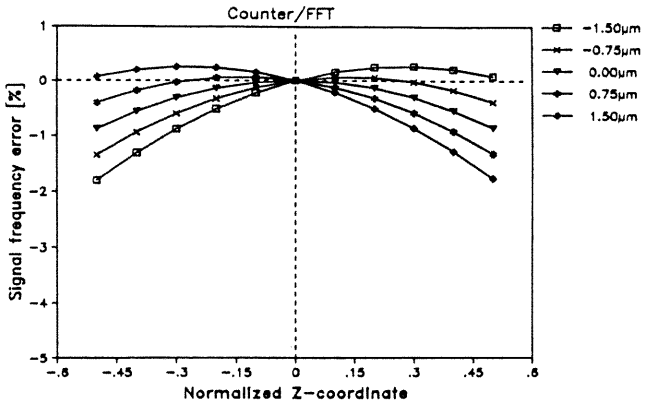

Figure 10: Estimated frequency error for Gaussian field distribution.

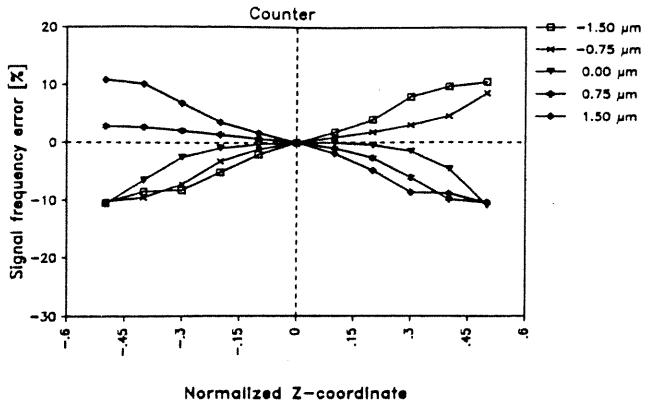

Figure 11: Estimated frequency error for Lorentzian distribution: counter processor.

The above-mentioned theoretical results were compared with experimental data. The anemometer used for this purpose had overall dimensions of 40 mm × 40 mm × 230 mm, which are obviously much smaller than an equivalent unit employing a gas laser and a photomultiplier tube. The optical data of the system are listed in Table 2. Some of the entries have two values: the first value is valid for evaluation with Lorentzian distribution in the plane of beam intersection, the second one is applicable when the beam splitter has been rotated 90°. In the latter case, a half-wave plate is used to rotate the polarization of the collimated beam by 90°. In this way, the beam splitter always receives the collimated beam with the same polarization and splits it effectively in two equal parts.

Laser diode	Hitachi HL 8314, Hitachi HL 8351
Power	30 mW, 50 mW
Wavelength	830 nm
Beam divergence:	
Parallel to junction	10°, 9°
Perpendicular to junction	27°
Focal lengths:	
Collimator	6.98 mm, 4.5 mm
Front lens	100 mm
Collimator N.A.	0.35, 0.47
Beam spacing	20 mm

Table 2: Specifications of the LDA system.

The measuring volume of the LDA system was scanned with a 2 μm pinhole mounted near the edge of a rotating disc of di-

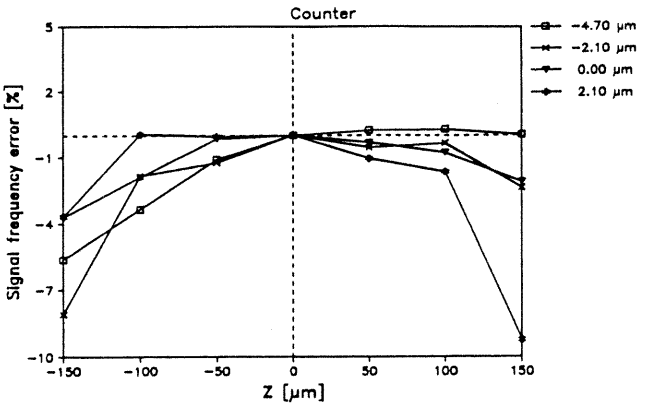

Figure 13: Measured frequency error for Lorentzian distribution: counter processor.

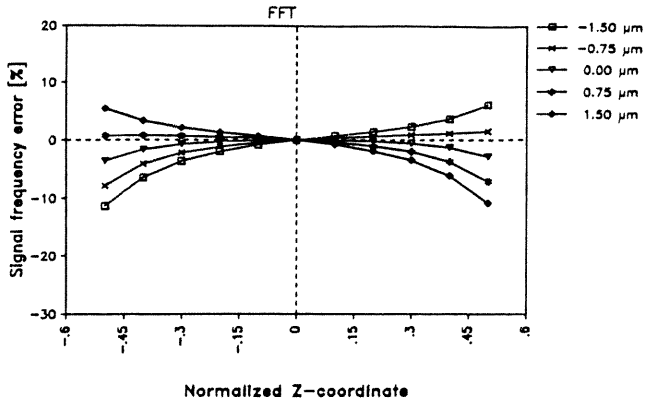

Figure 12: Estimated frequency error for Lorentzian distribution: burst spectrum analyzer.

ameter 90 mm. The speed of the motor, used to rotate the disc, was stabilized within 0.1%. The pinhole was traversed normal to the fringes. Precision translators were used to position the path of the pinhole within the measuring volume. The least count for the readout of the translator position was 0.1 μm and the specified accuracy of positioning was 0.02 μm.

The light transmitted through the pinhole during each scan was focused onto an APD which produced an electrical signal simulating a Doppler burst. The measured signal was transmitted to a digital oscilloscope and a counter-type LDA processor. Subsequently, the digitized burst was received by a microcomputer, which performed a fast Fourier transform (FFT) to determine the peak of the spectrum. The reported values of the Doppler frequency were deduced from averages of 20 scans at each measuring location. Typically, the r.m.s value over 20 scans has been less than 0.1% of the mean value.

For the cases of Lorentzian and Gausssian distributions lying in the plane of beam intersection, the counter processor yielded the signal frequency averaged over 4 cycles and 8 cycles respectively. Since the signals from the Lorentzian distribution have non-uniform periods, a tolerance of 4% between the frequencies of the first half and the entire signal was necessary for effective validation. For the Gaussian distribution, this tolerance limit was reduced to 1.5%. The value of average frequency was received by the microcomputer. An average of 1000 scans was taken at each location. The r.m.s value for these measurements was normally smaller than 0.5% of the mean. Only near the edges of the measuring volume, a significantly higher r.m.s value was observed.

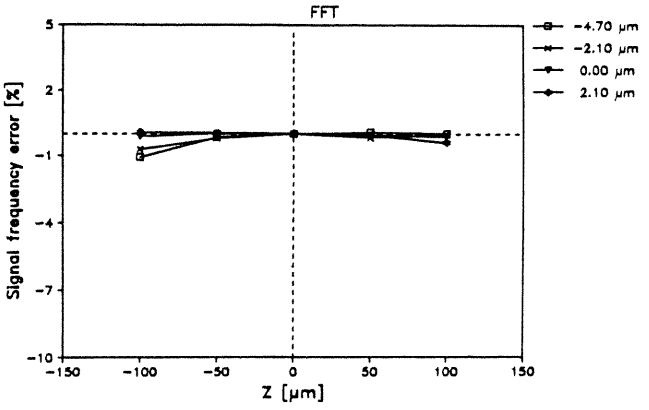

Figure 14: Measured frequency error for Lorentzian distribution: burst spectrum analyzer.

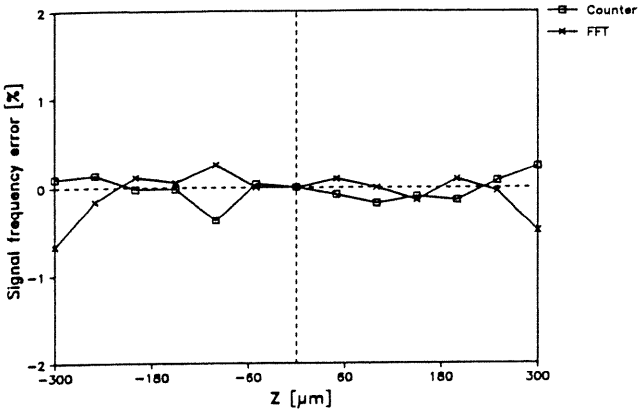

Figure 15: Measured frequency error for Gaussian distribution.

The values of measured relative error in the signal frequency are presented in Fig. 13 through 15. In the case of Lorentzian distribution, the errors are clearly suppressed with frequency-domain processing. The difference between the counter measurements and the FFT output is more pronounced than predicted. This effect may be attributed to aberration of the collimator which is not included in theoretical estimates. It is also due to collimator aberration that measured sensitivity of frequency errors to the collimator position is smaller than that predicted.

The Gaussian distribution has smaller divergence and hence, the aberration effects are not significant. As shown in Fig. 15, the measured values of frequency error are in agreement with the theoretical estimates. Also as predicted, there is no significant difference between the time-domain and frequency-domain signal processing.

In order to further illustrate the effects of fringe non-uniformity, some measurements were taken in a free jet in air, which are presented in Fig. 16 & 17. For these measurements, Lorentzian distribution was used in the plane of beam intersection. With optimal alignment, measurements were taken both in forward scatter and side scatter. The flow was seeded with micron-size water droplets and the signals were processed using a counter. For the measurement in side scatter, the length of the measuring volume was restricted to 100 μm.

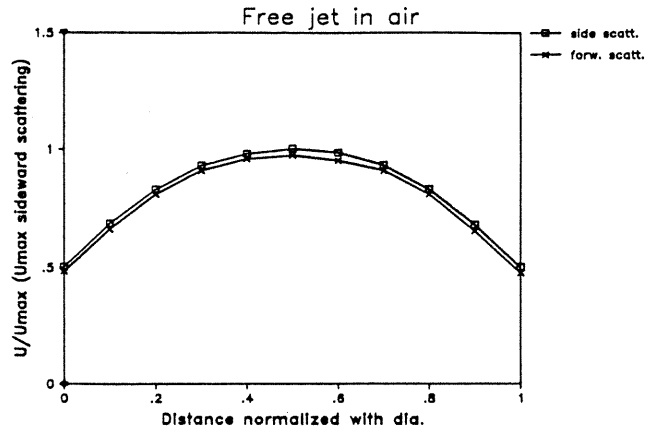

Figure 16: Mean velocity profile in a free jet.

As expected, the mean velocity measured in the forward scatter is smaller by about 3% than that measured in the side scatter. Hence, the calibration constant in forward scatter is larger than $\lambda / 2 \sin\theta$. For the applications involving a measurement of only mean flow speed in the forward scatter, such as a volume flow meter /20/, the calibration constant must be determined experimentally for accurate results.

The measured turbulence intensity is high in forward scatter and lies in the range expected from the results of the scanning experiments. In the side scatter, the measured turbulence is smaller than 1%, which is comparable with the results of conventional LDA measurements in a similar flow.

5. PDA-MEASUREMENTS IN SPRAYS

In principle, a number of the optical techniques can be extented to two-phase flow measurements. This will be explained for laser-Doppler anemometry which can be set up to analyze the radiation from small and large particles. If not only the frequency of the signal is interpreted, but also the phase difference between two photodetectors in space, information on the size of the particles can be obtained. In this way, particulate two-phase flow systems can be experimentally studied and results not obtainable with any other instrumentation may be deduced. Such data provide advanced information on particulate two-phase flows and lead to improved and advanced theoretical treatments of flows that are important in engineering practice.

In recent years, laser-Doppler anemometry was developed to be applied to particulate two-phase flows allowing measurements of particle velocity, fluid velocity, particle size and particle concentraction. Details of this extension of the LDA-measuring technique are given in references /21/ through /24/. The reader is referred to these references for further information regarding the development of the technique. To illustrate applications of this technique, a summary of the recent investigations on a water spray are given here. The spray was produced by a Danfoss 60° oil burner nozzle.

Since the size distribution is strongly dependent on the liquid and air properties and the pressures in the supply system, a special test rig was designed and built which allowed a careful control of the major parameters influencing the particle size in

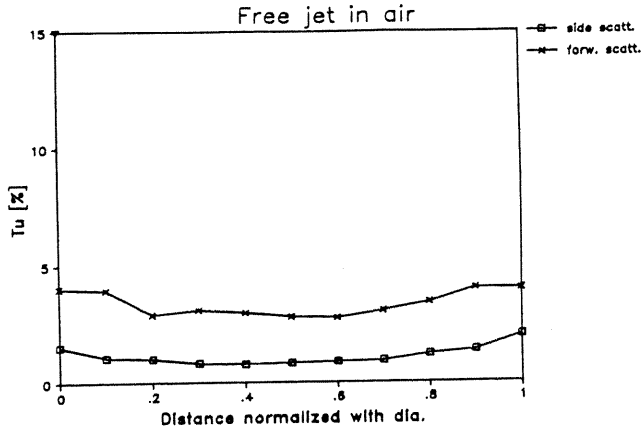

Figure 17: Turbulence intensity in a free jet.

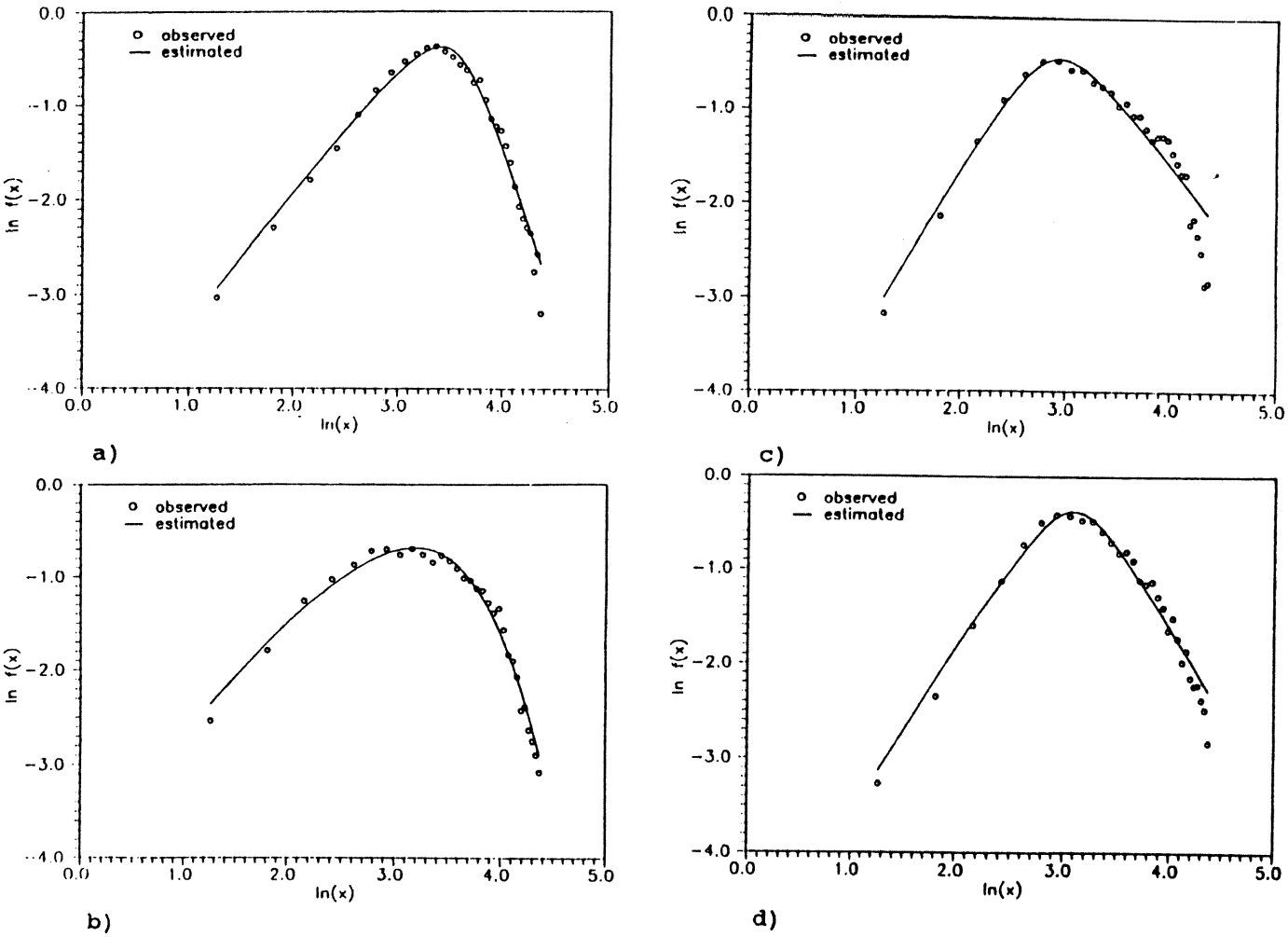

Figure 18: The log-density function of the fitted distribution at a distance (a) 15 mm, (b) 25 mm, (c) 50 mm, (d) 80 mm from the nozzle.

the spray. The main features of the experimental rig are listed below:

- 20 litre water storage tank,
- air supply system with pressure regulator to hold the pressure constant within ±1%,
- heating and cooling systems for temperature control to maintain these properties constant within ±1%,
- pressure and temperature sensors on the supply line near the nozzle,
- surrounding plexiglass tube (300 mm diam.) with connecting line to a ventilator,
- flow straightener to obtain a controlled air entrance to the flow chamber of the secondary air.

The nozzle, a Danfoss 60° solid cone house oil burner nozzle, was mounted on a straight metal pipe. This pipe was connected to a 3-D traversing mechanism, allowing accurate positioning of the nozzle relative to the spatially fixed optical system. The traverse of the optics was possible with an accuracy of approximately ±0.02 mm. This was considered sufficient for the present investigation. The experimental set-up was located inside of a laboratory which permitted the air properties, i.e., the temperature, humidity etc., to be held fairly constant during the experiments reported here. Temperature was found to be 20 °C±1 °C, and humidity around 50%. The water temperature at the nozzle exit was recorded to be between 15 °C and 17 °C.

The measuring system used in the present investigation was a so called phase-Doppler anemometer (PDA), a particle sizing technique based on laser- Doppler anemometry. It is now well known as a technique giving the temporal size distribution as well as the velocity of particles with a high spatial resolution and a very good accuracy, see Durst and Zaré /21/, Bauckhage and Flögel /22/, Bachalo and Houser /23/, Saffman et al. /24/.

The PDA system, developed and built at LSTM Erlangen had a measuring volume of approximately 1 × 0.2 × 0.2 mm. A 15 mW Helium-Neon laser was used as a light source which yielded sufficient scattering power for the drop sizes created by the nozzle. The receiving system consisted of a single light collecting lens, two focussing lenses and two avalanche photo diodes. The resultant signals were digitized by a 100 MHz transient recorder and subsequently processed in a computer by means of a data reduction code using Fourier transform as the basic method to obtain the phase difference between the signals. To measure the size distribution at one point in space, between 20,000 and 50,000 samples were taken, each individual measurement with a size error bound of ±3%. In that way, final results were obtained that possessed a high statistical reliability. This is indicated by the low scatter of the data points in the various diagrammes. After some initial measurements, the size range was found out to lie within 2.5 to 100 microns. To cover this entire range, the position of the two receiving lenses was altered in such a way that this size range was covered by 40 classes of particles.

Some of the results obtained in these investigations, using phase-Doppler anemometry as the measuring technique, are presented in Fig. 18(a)–(d). In reference /25/, more information is provided on these measurements and it is shown that the measured distributions can be well fitted by log-hyperbolic distributions. Detailed studies of these distributions has been possible because of the reliable measurements obtained by phase-Doppler anemometry.

It is to be expected that more optical techniques will be extended to two-phase flow measurements and, hence, fluid dynamics of two-phase flows in general and particulate two-phase flows in particular will be enhanced through new knowledge obtained with new or extended measuring techniques.

6. CONCLUSIONS

The present paper describes research and development work that was carried out at the institute of the authors in order to produce LDA- and PDA-systems that are suited to study flows in internal combustion engines. A compact fiber optical probe is described that uses graded index fibers to make up the optical measuring head. This is laid out for two-channel measurements and also contains the receiving optics. Using the glass fiber probe, in-cylinder measurements were taken under firing conditions. Valuable results were obtained from these measurements, providing an insight into the flows that occur during a full engine cycle. The measurements have shown that cycle-to-cycle variation in the pressure field are nearly uncorrelated with variations in the local velocity.

It is also pointed out in this paper that semi-conductor lasers are now becoming available that will permit development of miniaturized LDA-systems. LDA-measuring probes are foreseeable that would have the size of glass fiber probes as they are nowadays available. Such semi-conductor LDA-systems will contain the laser and the photo detector in the measuring head and will work in back scatter. Due to the low electrical energy requirements of semi-conductor lasers, these systems would be suitable for in-cylinder measurements during road tests on automobiles.

Both glass fiber optics and semi-conductor laser systems can be extended to build phase-Doppler anemometers that can be utilized to study size and velocity distributions in sprays. Such a system was set up and a spray study was carried out. It was shown that a large amount of data result that need to be reduced, in order to be used for practical purposes. Data reduction can be achieved by fitting analytical functions to the measured distributions. The authors' studies have shown that the log-hyperbolic distribution provides excellent fitting to the data. Parameters of this function can be utilized to study the effects of spray nozzle geometry, liquid properties, supply pressure, etc., on sprays. This has been demonstrated and extensive descriptions are available in other publications of the authors and their colleagues.

REFERENCES

1. Rask, R.B.: Laser Doppler Measurements in an Internal Combustion Engine, *SAE Paper 790094* (1979) 1–12.
2. Wigley, G.; Glanz, R.: A Laser Anemometer System for Engine Flow Studies, *2nd Int. Symp. on Appl. of Laser Anemom. to Fluid Mech., Lisbon* (1984) 9.3.
3. Fansler, T.D.: Laser Velocimetry Measurements of Swirl and Squish Flows in an Engine with a Cylindrical Piston Bowl, *SAE Paper 850124* (1985).
4. Bopp, S.; Vafidis, C.; Whitelaw, J.H.: The Effect of Engine Speed on the TDC Flow Flied in a Motored Reciprocating Engine, *SAE Paper 860023* (1986).
5. Hall, M.J.; Bracco, F.V.; Santavicca, D.A.: Cycle-Resolved Velocity and Turbulence Measurements in an IC Engine with Combustion, *SAE Paper 860320* (1986) 1–12.
6. Foster, R.E.; Witze, P.O.: Two-Component Laser Velocimeter Measurements in a Spark Ignition Engine, *Combst. Sci. and Tech.*, **59** (1988) 85–105.
7. Dantec Elektronik: Fiber Flow Anemometers, Product Catalogue (1988).
8. TSI Inc.: Colour Burst Multicolor Beam Separator, Data Sheet (1989).
9. Obokata, T.; Hanada, N.; Kurabayashi, T.: Velocity and Turbulence Measurements in a Combustion Chamber of S.I. Engine Under Motored and Firing Operations by LDA with Fiber Optic Pick-up, *SAE Paper 870166* (1987).
10. Durst, F.; Krebs, H.; Weber, H.: Entwicklung von miniaturisierten Laser-Doppler-Optiken für Messungen in Motoren, *Automobile-Industrie*, **3** (1985) 327–334.
11. Dopheide, D.; Taux, G.; Reim, G.; Faber, M.: Laser Doppler anemometry using laser diodes and solid-state photodetectors, *Proc. 3rd. Int. Symposium on Laser Anemometry, Lisbon* (1986) 8.2.
12. Brown, R.G.W.; Burnett, J.G.; Hackney, N.: A Miniature, Battery Operated Laser Doppler Anemometer, *Proc. 4th. Int. Symposium on Laser Anemometry, Lisbon* (1988) 3.4.
13. Dopheide, D.; Faber, M.; Reim, G.; Taux, G.: A Portable Frequency Stabilized Laser Diode Backscatter Semiconductor LDA for High Velocity Applications, *Proc. 4th. Int. Symposium on Laser Anemometry, Lisbon* (1988) 4.4.
14. Damp, S.: Battery Driven Miniature LDA System with Semiconductor Laser Diode, *Proc. 4th. Int. Symposium on Laser Anemometry, Lisbon* (1988) 5.4.
15. Bopp, S.: Strömungsmechanische Untersuchungen in Motoren mittels Laser Doppler Glasfasersonden, Dissertation, Univ. Erlangen-Nuremberg (1990).
16. Lorenz, M.; Prescher, K.: Cycle-Resolved LDV Measurements on a Fired SI-Engine at High Data Rates Using a Conventional Modular LDA System, *SAE Paper* (1990).
17. Hanson, S.: Broadening of measured frequency spectrum in a differential laser anemometer due to interference plane gradients, *J. Pys. D*, **6** (1973) 164–171.

18. Durst, F.; Stevenson, W.H.: Influence of Gaussian beam properties on laser Doppler signals, *Applied Optics*, **18** (1979) 516–524.

19. Müller, R.; Naqwi, A.: Optimization of a Laser Diode Anemometry System, Report LSTM 239/T /88, Universität Erlangen, F.R. Germany (1988).

20. Durst, F.; Bopp, S.; Brunn, P.O.; Holweg, H.; Weber, H.: An Optical Sensor for Accurate, Small Volume Rate Measurements, *Sensor 88, Nürnberg*, Congress Proceedings (1988) 161–185.

21. Durst, F.; Zaré, M.: Laser Doppler Measurements in Two-Phase Flows, *LDA-Symposium, Copenhagen*, Congress Proceedings (1975) 403–429.

22. Bauckhage, K.; Flögel, H.-H.: Simultaneous Measurements of Droplets Size and Velocity in Nozzle Sprays, *Proc. 2nd Intl. Symp. on Appl. Laser Anemometry to Fluid Mechanics, Lisbon*, (1984).

23. Bachalo, W.D.; Houser, M.J.: Phase/Doppler Spray Analyzer for Simultaneous Measurements of Drop Size and Velocity Distributions, *Optical Engineering*, **23** (1984) 583–590.

24. Saffman, M.; Buchhave, P.; Tanger, H.: Simultaneous Measurements of Size, Concentration, and Velocity of Spherical Particles by a Laser Doppler Method, *Proc. 2nd Intl. Symposium on Appl. of Laser Anemometry to Fluid Mechanics, Lisbon*, (1984).

25. Bhatia, J.C.; Domnick, J.; Durst, F.; Tropea, C.: Phase-Doppler Anemometry and the Log-Hyperbolic Distribution Applied to Liquid Sprays, *Part. Part. Syst. Charact.*, **5** (1988) 153–164.